**The EMBO Journal (2010) 29,** 2827–2840 | © 2010 European Molecular Biology Organization | All Rights Reserved 0261-4189/10
www.embojournal.org

THE EMBO JOURNAL

# PTEN is recruited to the postsynaptic terminal for NMDA receptor-dependent long-term depression

**Sandra Jurado[1,3], Marion Benoist[2], Argentina Lario[2], Shira Knafo[2], Cortney N Petrok[1] and José A Esteban[2,*]**

[1]Department of Pharmacology, University of Michigan Medical School, Ann Arbor, MI, USA and [2]Department of Neurobiology, Centro de Biología Molecular 'Severo Ochoa', Consejo Superior de Investigaciones Científicas (CSIC), Madrid, Spain

**Phosphatase and tensin homolog deleted on chromosome ten (PTEN) is an important regulator of phosphatidylinositol-(3,4,5,)-trisphosphate signalling, which controls cell growth and differentiation. However, PTEN is also highly expressed in the adult brain, in which it can be found in dendritic spines in hippocampus and other brain regions. Here, we have investigated specific functions of PTEN in the regulation of synaptic function in excitatory hippocampal synapses. We found that NMDA receptor activation triggers a PDZ-dependent association between PTEN and the synaptic scaffolding molecule PSD-95. This association is accompanied by PTEN localization at the postsynaptic density and anchoring within the spine. On the other hand, enhancement of PTEN lipid phosphatase activity is able to drive depression of AMPA receptor-mediated synaptic responses. This activity is specifically required for NMDA receptor-dependent long-term depression (LTD), but not for LTP or metabotropic glutamate receptor-dependent LTD. Therefore, these results reveal PTEN as a regulated signalling molecule at the synapse, which is recruited to the postsynaptic membrane upon NMDA receptor activation, and is required for the modulation of synaptic activity during plasticity.**

*The EMBO Journal* (2010) **29,** 2827–2840. doi:10.1038/emboj.2010.160; Published online 13 July 2010
*Subject Categories*: membranes & transport; neuroscience
*Keywords*: AMPA receptors; hippocampus; LTD; NMDA receptors; spines

## Introduction

Phosphatase and tensin homolog deleted on chromosome ten (PTEN; also known as MMAC1 or TEP1) was originally cloned as a tumour suppressor protein (Li *et al*, 1997; Steck *et al*, 1997). PTEN antagonizes phosphatidylinositol-3′-kinase (PI3K) signalling by dephosphorylating phosphatidylinositol-(3,4,5,)-trisphosphate ($PIP_3$) to generate phosphatiylinositol-(4,5)-bisphosphate ($PIP_2$) (Maehama and Dixon, 1999). As a negative regulator of the PI3K-$PIP_3$ pathway, PTEN restrains cell proliferation and survival during embryogenesis. Consistent with this developmental function, PTEN *null* mice die during embryogenesis, whereas heterozygotes are tumour prone and display enlargement of multiple organs (Stiles *et al*, 2004). Similarly, alterations in the function of PTEN are of major relevance for the incidence of a wide variety of human cancers (Li *et al*, 1997; Pendaries *et al*, 2003).

In the central nervous system, PTEN is expressed in most, if not all neurons. It is present in dendrites and spines of cerebral cortex, cerebellum, hippocampus and olfactory bulb (Perandones *et al*, 2004). Mutation or inactivation of PTEN contributes to brain tumours, macrocephaly, seizures and ataxia (Backman *et al*, 2001; Kwon *et al*, 2001; Eng, 2003). PTEN mutations have been also associated with mental retardation and autism spectrum disorders (Butler *et al*, 2005; Kwon *et al*, 2006). At the cellular level, neurons lacking PTEN develop larger and more branched dendrites, which harbour more synapses (Jaworski *et al*, 2005; Kwon *et al*, 2006; Fraser *et al*, 2008). Therefore, it is likely that the neurological deficits associated to PTEN mutations are derived from aberrant neuronal growth and connectivity during brain development. These widespread morphological changes may also be the reason for the pleiotropic effects on synaptic function and plasticity that have been reported for mice with reduced PTEN expression (Wang *et al*, 2006; Fraser *et al*, 2008).

Besides these developmental aspects, the $PIP_3$ pathway has specific functions at synapses in differentiated neurons. For example, acute blockade of PI3K, the $PIP_3$ synthesizing enzyme, has been shown to impair some forms of memory formation (Chen *et al*, 2005) and long-term potentiation (LTP) in hippocampal slices (Sanna *et al*, 2002; Tang *et al*, 2002; Cammalleri *et al*, 2003; Opazo *et al*, 2003). The $PIP_3$ pathway has also been linked to AMPAR trafficking (Qin *et al*, 2005) and synaptic localization (Arendt *et al*, 2010) in hippocampal neurons. However, a specific function for PTEN in synaptic transmission or plasticity in developed neurons has not been pinpointed yet.

From a mechanistic point of view, PTEN possesses a PDZ-binding motif at its C-terminus (residues $Thr^{401}$-$Lys^{402}$-$Val^{403}$-COOH), which interacts with multiple PDZ domain-containing proteins, such as the scaffolding proteins MAGI-1/2/3, hDlg/SAP97 and the Ser/Thr kinase MAST205 (Bonifant *et al*, 2007). The physiological consequences of these PDZ-dependent interactions remain poorly characterized; however, it has been shown that the binding of PTEN to specific PDZ domain-containing proteins contributes to PTEN protein stability (Valiente *et al*, 2005). Nevertheless, no interaction between PTEN and synaptic PDZ proteins has been reported yet.

In this study, we have investigated specific functions of PTEN in synaptic plasticity, separate from its developmental

*Corresponding author. Department of Neurobiology, Centro de Biología Molecular 'Severo Ochoa', Consejo Superior de Investigaciones Científicas (CSIC), Nicolas Cabrera 1, Madrid 28049, Spain.
Tel.: +34 91 196 4637; Fax: +34 01 196 4420;
E-mail: jaesteban@cbm.uam.es
[3]Present address: Department of Psychiatry and Behavioral Science, Stanford School of Medicine, Palo Alto, CA 94304, USA

**Received: 14 September 2009; accepted: 24 June 2010; published online: 13 July 2010**

functions. In particular, we have found that NMDA receptor activation triggers the association between PTEN and postsynaptic density-95 (PSD-95) through a PDZ-dependent interaction. This interaction leads to the recruitment and anchoring of PTEN to the postsynaptic membrane, and possibly mediates a specific function of PTEN in the expression of long-term depression (LTD). These results have revealed PTEN as a regulated component of the intracellular signalling machinery that controls synaptic transmission and plasticity at hippocampal excitatory synapses.

## Results

### *NMDA receptor activation regulates a PDZ-dependent association between PTEN and PSD-95*

As an initial step to evaluate potential functions of PTEN at synapses, we tested its association with PSD-95, a critical regulator of synaptic function and plasticity (El-Husseini *et al*, 2000; Ehrlich and Malinow, 2004; Bhattacharyya *et al*, 2009). To this end, we immunoprecipitated PTEN from total hippocampal extracts, and the presence of co-immunoprecipitated proteins was analysed by western blot (see Materials and methods). As shown in Figure 1A (upper panels, 'Control' lanes), there was a detectable association between PSD-95 and PTEN, which was specific, according to the immunoprecipitation with a non-immune ('n.i.') antibody. Interestingly, the association between PSD-95 and PTEN appeared to be regulated by activity, as it was increased after 5 min bath application of 20 μM NMDA (Figure 1A, compare 'Control' and 'NMDA' lanes), and this increase was abolished by incubation with the NMDAR antagonist AP5 (Figure 1B, 'NMDA + AP5' lanes). There was also a weak, but detectable, interaction between PTEN and MAGI-2, another PDZ protein known to associate with PTEN (Wu *et al*, 2000). However, this interaction was not altered by NMDAR activation (Figure 1A, middle panels).

We then tested whether the association between PSD-95 and PTEN was specifically regulated by NMDAR activation or whether it could also be induced by other forms of neuronal activation or depolarization. To this end, we compared the amount of PTEN-PSD-95 co-immunoprecipitation from slices incubated for 5 min with NMDA (20 μM), AMPA (100 μM) or KCl (50 mM). A control immunoprecipitation with an n.i. antibody was also carried out. Interestingly, the association between PTEN and PSD-95 was only enhanced in slices treated with NMDA, but not with AMPA or KCl (Figure 1C, right panel; total protein inputs for all conditions are shown in the left panel). To evaluate the time course of this association, we carried out immunoprecipitations at different times after the 5 min incubation with NMDA. As shown in Figure 1D and E, the association between PTEN and PSD-95 persists for a period of time after the end of NMDAR activation, although it gradually declines by the end of the time course. It should also be pointed out that the fraction of PSD-95 associated with PTEN is rather low at all times: around 1% of the total PSD-95 under basal conditions, roughly doubling after NMDA induction (see quantification in Figure 1E). The regulated association between PSD-95 and PTEN was also observed after immunoprecipitation of PSD-95 and detection of PTEN as a co-precipitated protein (Supplementary Figure 1). This regulation appears to be specific for PTEN, because the interaction of PSD-95 with another PDZ-dependent partner (the NMDA receptor) was not enhanced by this treatment (Supplementary Figure 1, PTEN versus GluN1 panels).

To further characterize the structural requirements of this regulated association between PSD-95 and PTEN, we expressed GFP-tagged PTEN in organotypic slice cultures of rat hippocampus for 15–20 h (GFP is fused to the N-terminus of PTEN). Confocal imaging of infected CA1 neurons showed widespread distribution of GFP-PTEN, including distal dendrites and spines (Figure 1F). Recombinant GFP-PTEN was functional, as evidenced from its ability to antagonize the PI3K/$PIP_3$ pathway, leading to a decrease in Akt phosphorylation at Ser473 (Stambolic *et al*, 1998) (Supplementary Figure 2A and B). Total protein extracts were prepared from untreated slices or from slices treated with NMDA, AMPA or KCl, as described above. Immunoprecipitations were carried out with an anti-GFP antibody, and the immunoprecipitated fractions were analysed by western blot. As shown in Figure 1G, PSD-95 was co-precipitated with GFP-PTEN only after NMDAR activation, but not after AMPA or KCl treatment, similar to the results obtained with endogenous PTEN (Figure 1C). The kinetics of GFP-PTEN association with PSD-95 were also similar to the endogenous protein (Figure 1H, right panels; inputs for all conditions are shown in the left panels). As control, cytosolic GFP did not co-immunoprecipitate with PSD-95 with or without NMDA (Figure 1H).

### *PDZ-dependent interactions anchor PTEN at dendritic spines upon NMDA receptor activation*

To determine whether the association between PTEN and PSD-95 was PDZ dependent, we generated a PTEN mutant lacking the last four amino acids, which contain the PDZ ligand motif (-ITKV*). We then carried out co-immunoprecipitations from slices expressing GFP, full-length GFP-PTEN or the truncated form of PTEN lacking its PDZ-binding motif (GFP-PTEN-ΔPDZ) (see Supplementary Figure 2C for a western blot analysis of the expression of this and other PTEN derivatives used in this study). As shown in Figure 2A (upper right panel), the association with PSD-95 was only detectable with GFP-PTEN, but not with GFP-PTEN-ΔPDZ or cytosolic GFP, and only after NMDAR activation. This result confirms that the association between PTEN and PSD-95 requires the PDZ motif at the PTEN C-terminus.

PSD-95 is a well-known synaptic scaffolding molecule that organizes multiple signalling complexes at the synapse (Sheng, 2001). Therefore, our biochemical results described above suggest that PTEN may be recruited and anchored at synapses after NMDAR activation. To test this possibility, we evaluated real-time dynamics of PTEN in dendritic spines using fluorescence recovery after photobleaching (FRAP; see fluorescence images from a representative experiment in Figure 2B). GFP-tagged PTEN was expressed in organotypic hippocampal slices, and the NMDA treatment was carried out as described above. Spines expressing GFP-PTEN were photobleached and the extent of fluorescence recovery was measured before and after NMDAR activation ('+5', '+15' and '+25' min; for simplicity, the '+15-min' time point is only shown in the summary Figure 2F). As shown in Figure 2C (white circles), approximately 50% of the GFP-PTEN signal is recovered in the spine over a time course of 10–20 s, arguing that 50% of GFP-PTEN is stable in spines (over this period of time) under basal conditions. Intriguingly, GFP-PTEN fluorescence recovered to a significantly greater extent (around

 

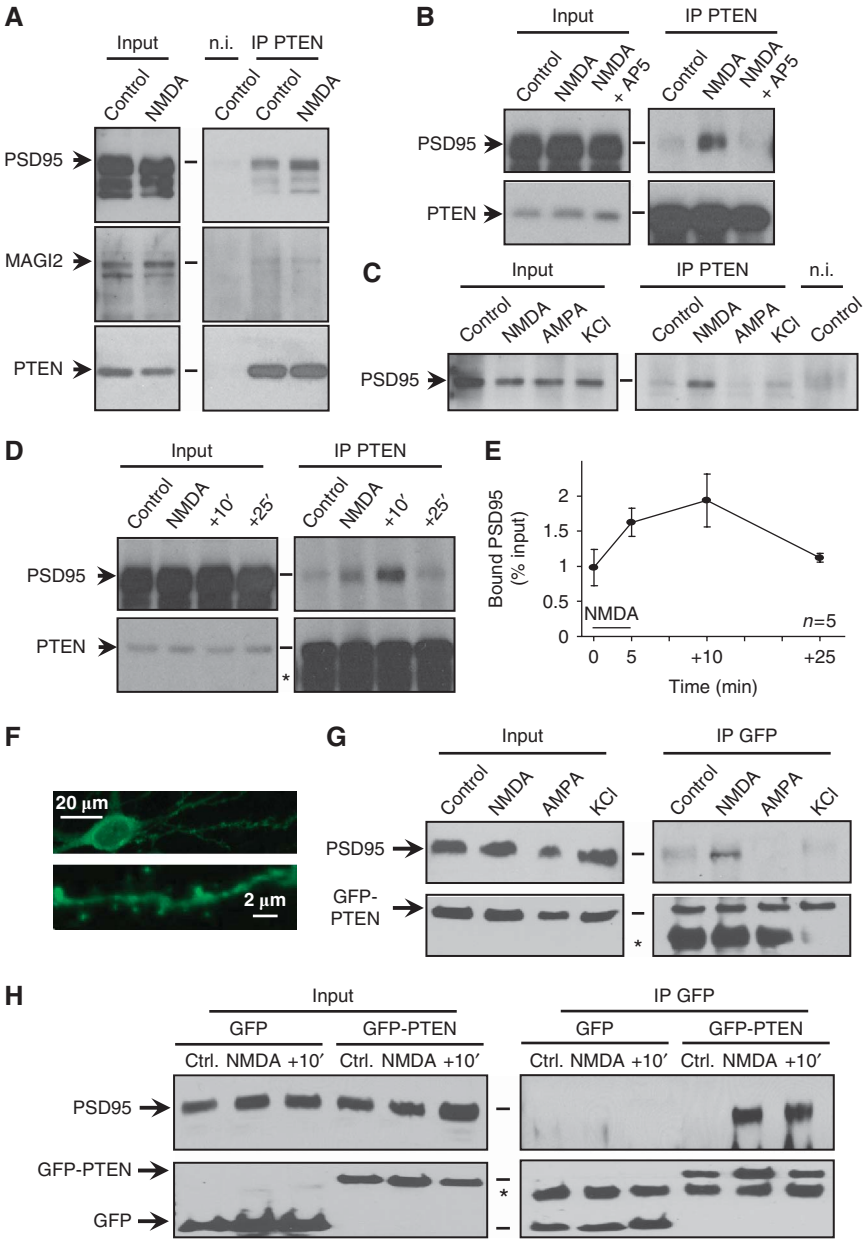


**Figure 1** NMDA receptor-dependent association between PTEN and PSD-95. (**A**) Total protein extracts from hippocampal slices were immunoprecipitated with anti-PTEN or with a non-immune ('n.i') antibody ('Control' lanes). Some slices were treated with 20 μM NMDA for 5 min before the immunoprecipitation ('NMDA' lanes). For all western blots, immunoprecipitated proteins are shown in the right panels, and 10% of the inputs in the left panels. (**B**) Similar to (**A**), but some slices were preincubated with the NMDAR antagonist AP5 before and during the NMDA treatment ('NMDA + AP5'). (**C**) Similar to (**A**), with slices treated for 5 min with 20 μM NMDA, 100 μM AMPA, 50 mM KCl or left untreated ('Control'), as indicated. (**D**) Similar to (**A**), with untreated slices ('Control'), treated with 20 μM NMDA for 5 min ('NMDA') or transferred to regular ACSF for 10 min (+10′) or 25 min (+25′) after the NMDA treatment. Asterisk (*) indicates the position of the IgG used for immunoprecipitation. (**E**) Quantification of the fraction of PSD-95 co-precipitated with PTEN (as percentage from the total PSD-95 amount in the input), from five independent experiments as the one shown in (**D**). The 5 min NMDA treatment is represented with a black bar. (**F**) Representative confocal image showing the distribution of recombinant GFP-PTEN in soma, dendrites and spines in a hippocampal neuron from organotypic slice cultures. (**G**) Hippocampal slices expressing GFP-PTEN were treated for 5 min with 20 μM NMDA, 100 μM AMPA, 50 mM KCl or left untreated ('Control'), as indicated. Total protein extracts were immunoprecipitated with anti-GFP and analysed by western blot with anti-PSD-95 (upper panels) or anti-GFP antibodies (lower panels). Asterisk (*) indicates the position of the IgG used for immunoprecipitation. (**H**) Hippocampal slices expressing GFP or GFP-PTEN, as indicated, were left untreated ('Ctrl.'), or were treated with 20 μM NMDA for 5 min ('NMDA'), or were transferred to regular ACSF for 10 min after the NMDA treatment (+10′). Total protein extracts were immunoprecipitated with anti-GFP and analysed as in (**G**). Asterisk (*) indicates the position of the IgG used for immunoprecipitation.

70%) 5 min after the NMDA treatment (Figure 2C, red circles). This result indicates an increase in PTEN mobility rapidly after NMDAR activation. In contrast, 20–30 min after the NMDA treatment, the recovery of fluorescence of GFP-PTEN in the spine was drastically reduced (around 20%; Figure 2C, dark red circles; Figure 2F), implying that a larger fraction of PTEN is retained in spines in a long-lasting manner after NMDAR activation.

To test the function of PDZ interactions in this behaviour, we carried out similar experiments with the truncated form of

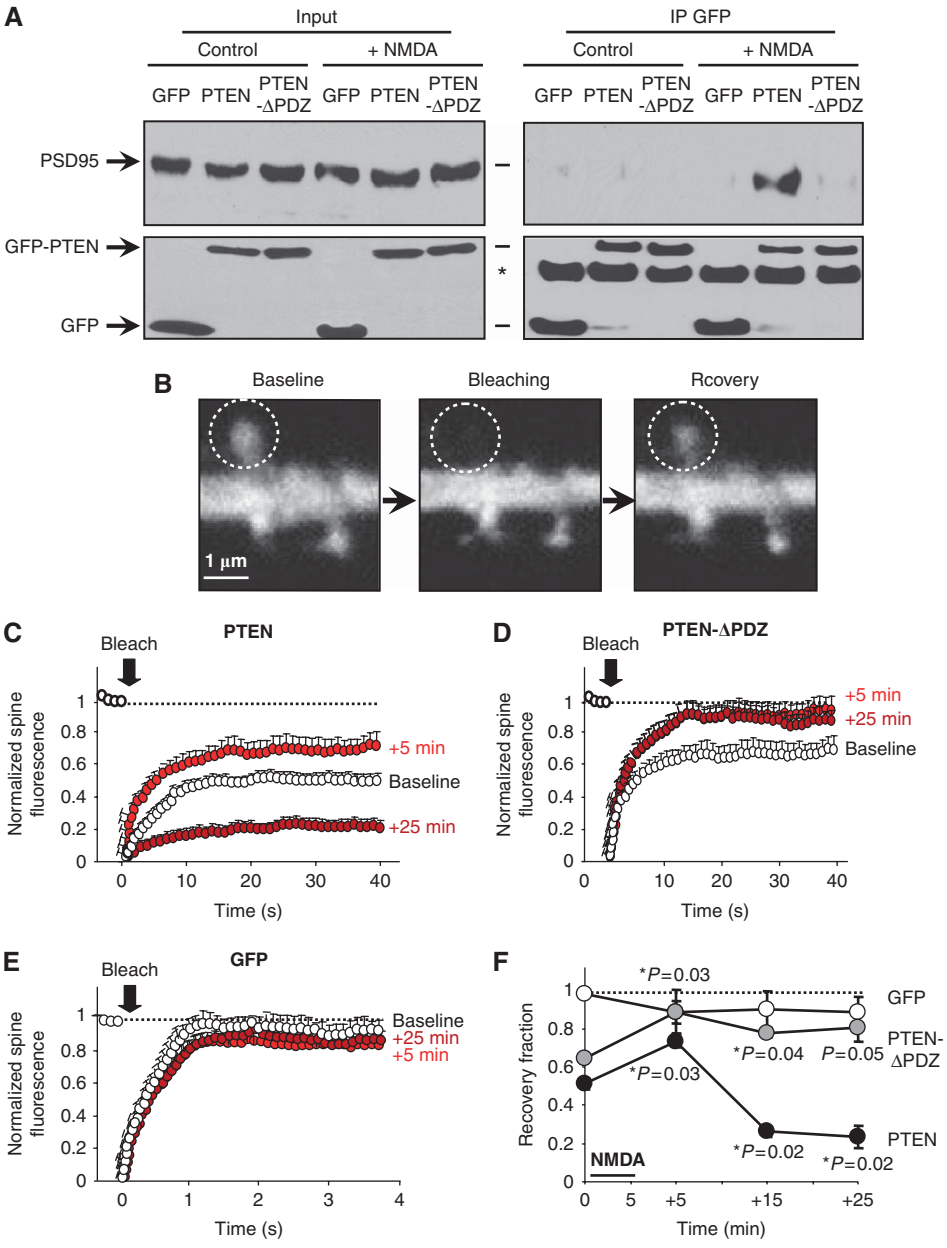


**Figure 2** PDZ-dependent interactions and anchoring of PTEN in spines. (**A**) Coimmunoprecipitation experiments were similar to those in Figure 1H, with slices expressing GFP, GFP-PTEN or the PDZ truncated mutant GFP-PTEN-ΔPDZ. Slices were treated with 20 μM NMDA for 5 min (' + NMDA') or left untreated ('Control'). Western blot is representative of three independent experiments. (**B**) Representative confocal images from an FRAP experiment. Left panel ('baseline') shows GFP-PTEN expression in a dendritic branch and its spines. A specific spine (white dashed circle) was bleached ('bleaching') and its fluorescence partially recovered 40 s later ('recovery'). (**C**) Quantitative analysis of FRAP experiments as the one shown in (**B**). 'Baseline' (white symbols) represents FRAP experiments on GFP-PTEN-expressing slices perfused with ACSF (untreated). The perfusion solution was then switched to ACSF containing 20 μM NMDA; 5 min later, the slices were washed again with standard ACSF. Further FRAP images were acquired after 5, 15 and 25 min of ACSF wash (' + 5 min', red symbols; ' + 25 min', dark red symbols; the ' + 15 min' time courses are similar to the ' + 25 min' ones and are only represented in the summary plot in (**F**), for simplicity). GFP fluorescence in the spine was normalized to the fluorescence in the unbleached dendritic shaft to correct for ongoing bleaching during imaging. Average values ± s.e.m. are plotted normalized to the baseline before bleaching. Number of spines analysed were 12 ('baseline'), 8 (' + 5 min') and 9 (' + 25 min') (different spines are imaged at each time point). (**D**, **E**) Similar to (**C**), with slices expressing GFP-PTEN-ΔPDZ (D) or plain GFP (**E**). Number of spines analysed for GFP-PTEN-ΔPDZ were 7 at each time point, and for GFP 6 ('baseline'), 5 (' + 5 min') and 5 (' + 25 min'). (**F**) Recovery fractions from experiments shown in (**C**–**E**) were calculated from the fraction of fluorescence recovered 40 s (GFP-PTEN and GFP-PTEN-ΔPDZ) or 4 s (GFP) after photobleaching. These values are plotted for untreated slices (0 min) or at different times after the 5 min NMDA treatment (the ' + 15 min' is not plotted in panels (**C**–**E**) for simplicity). Average values ± s.e.m. are plotted for GFP-PTEN (black symbols), GFP-PTEN-ΔPDZ (grey symbols) and GFP (white symbols). Statistical significance was calculated with respect to the recovery fractions before NMDA treatment. There was no significant difference in the case of GFP-expressing neurons.

PTEN lacking the PDZ motif, GFP-PTEN-ΔPDZ. As shown in Figure 2D, the extent of fluorescence recovery was also greater 5 min after NMDAR activation (60% at baseline—white circles—versus 90% 5 min after the NMDA treatment—red circles). But in marked contrast with full-length PTEN, this increase in PTEN mobility was long lasting (20–30 min

 

after the NMDA treatment) and was never followed by an enhanced retention in spines (Figure 2D, dark red circles; Figure 2F).

As a control for potential changes in fluorophore diffusion in spines as a result of NMDA application, we carried out similar NMDA-FRAP experiments in slices expressing GFP. As shown in Figure 2E and F, fluorescence recovery was nearly complete for GFP and was not altered at any time point in response to the NMDA treatment. In addition, neither the rates of recovery nor the net distribution between spines and dendrites were significantly altered for any of the recombinant proteins after the NMDA treatment (Supplementary Figure 3A and B, respectively).

Therefore, we conclude that NMDAR activation triggers a biphasic regulation of PTEN mobility in dendritic spines. First, there is a rapid and transient increase in mobility, which is independent from PDZ interactions. This phase is then followed by a longer-lasting and PDZ-dependent anchoring of PTEN at the spine (Figure 2F).

### *Biochemical association of PTEN with the PSD after NMDA receptor activation*

To further investigate the recruitment of PTEN to the postsynaptic machinery upon NMDAR activation, we evaluated its association with the PSD using standard fractionation methods (Carlin *et al*, 1980). To this end, we isolated synaptosomal fractions from 3 to 4 weeks rats (see Supplementary data). NMDARs were then activated on the purified synaptosomes by adding 20 μM NMDA and 10 μM glycine. After 5 min incubation, NMDAR activation was stopped with AP-5 and synaptosomes were incubated for 10 min more to allow for PTEN stabilization. Then, the PSD fraction was isolated as a Triton-insoluble pellet from treated and untreated synaptosomes and was analysed by western blot (see Supplementary data).

As shown in Figure 3, the abundance of PTEN at the PSD was significantly enhanced (two-fold) on the synaptosomes treated with NMDA plus glycine. The PSD enrichment of other postsynaptic markers was not altered (PSD-95) or was slightly decreased (GluN1 and αCaMKII) with this treatment, ruling out potential artefacts because of non-specific protein aggregation or precipitation. In conclusion, these experiments indicate that PTEN biochemically associates with the PSD scaffold after NMDAR activation, in agreement with its co-precipitation with the PSD-95 protein complex.

### *Local redistribution of PTEN within dendritic spines in response to NMDAR activation*

To directly visualize the recruitment of PTEN to the postsynaptic scaffold, we evaluated the ultrastructural localization of endogenous PTEN within dendritic spines before and after NMDA treatment. PTEN has been described to be present in axonal and dendritic compartments in hippocampal neurons (Perandones *et al*, 2004), but the fine-scale distribution of PTEN in dendritic spines had never been evaluated before.

We characterized the ultrastructural distribution of endogenous PTEN in close proximity to synaptic sites using postembedding immunogold electron microscopy (see Materials and methods; Figure 4A for representative micrographs). Most synaptic PTEN immunolabelling was found in the postsynaptic terminal (70% versus 30% presynaptic; Figure 4B). Within the postsynaptic compartment, PTEN labelling was predominantly located in the intracellular space of the spine (Figure 4B, 'Intra'), outside of the PSD and the extrasynaptic membrane ('Extra').

Remarkably, upon NMDAR activation (25 min after the NMDA treatment), PTEN fraction in the PSD increased by six-fold, whereas the amount of PTEN in other synaptic compartments was not significantly affected (Figure 4B, black columns; representative micrographs in Figure 4A). In addition, and consistent with this redistribution of PTEN into the PSD, we observed a global shift in the population of PTEN molecules towards the PSD (Figure 4C).

Therefore, and in agreement with our biochemical and fluorescence imaging data, these data confirm that endogenous PTEN redistributes to the postsynaptic membrane in response to NMDAR activation.

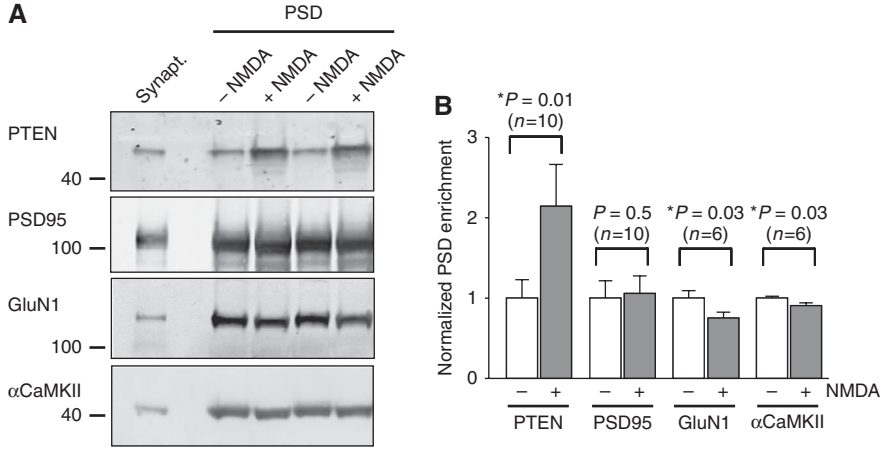


**Figure 3** Enrichment of PTEN at the postsynaptic density fraction after NMDA receptor activation. (**A**) Representative western blot analysis of PSD fractionations from synaptosomal preparations after NMDA receptor activation ('+NMDA') or untreated controls ('−NMDA'). A duplicate of separately treated or untreated samples is presented. The starting material (synaptosomal fraction) is shown in the left lane. (**B**) Quantification of PSD enrichment in NMDA-treated samples normalized to the untreated controls, from experiments as the one shown in (**A**); '*n*' represents number of independent experiments. Statistical significance was determined according to the Wilcoxon's test for pairs of treated–untreated samples.

### *Enhancement of PTEN activity depresses AMPA receptor-mediated synaptic transmission*

As an initial step to examine PTEN function in synaptic transmission, we overexpressed wild-type GFP-PTEN or a catalytically dead mutant (GFP-PTEN-C124S) in CA1 neurons from organotypic slice cultures. Importantly, expression of this mutant produced an increase in phospho-Akt over basal levels (Supplementary Figure 2A and B), indicating that this construct behaves as a dominant negative against endogenous PTEN activity in neurons, as it has been described earlier in other cell types (Maehama and Dixon, 1998).

The effect of GFP-PTEN and GFP-PTEN-C124S on synaptic transmission was evaluated by simultaneous double whole-cell recordings from pairs of nearby infected and uninfected CA1 neurons, under voltage-clamp configuration, while stimulating presynaptic Schaffer collateral fibres (to note, under this configuration, the recombinant proteins are always expressed exclusively in the postsynaptic neuron). As shown in Figure 5A–C, PTEN overexpression produced a significant depression of AMPAR-mediated currents as compared with uninfected cells, whereas NMDAR responses remained unchanged. In contrast, the catalytically dead mutant, PTEN-C124S, did not alter AMPAR- or NMDAR-mediated transmission (Figure 5D–F). This result verifies that the catalytic activity of PTEN is required for the depression of AMPAR-mediated transmission and that this is not due to virus infection or non-specific sequestration of regulatory proteins. Importantly, passive membrane properties, such as input resistance and holding current (related to basal ionic conductances), and whole-cell capacitance (related to cell size) were also similar in control and in PTEN-overexpressing neurons (Supplementary Figure 4).

Intriguingly, the depression of AMPAR responses produced by overexpression of PTEN was observed for basal synaptic transmission, that is conditions under which PTEN is not normally recruited to the postsynaptic membrane (earlier biochemical and imaging experiments). One possible explanation is that overexpressed PTEN is able to reach the postsynaptic membrane in the absence of its regulated association with PDZ proteins at the postsynaptic scaffold. To test this possibility, we carried out similar recordings with neurons overexpressing the truncated PTEN mutant lacking the PDZ motif (PTEN-ΔPDZ). As shown in Figure 5G–I, overexpressed PTEN was able to depress AMPAR responses in the absence of PDZ-dependent interactions. This depression was still specific for AMPARs, as compared with NMDARs. Therefore, although the recruitment of PTEN to the synaptic scaffold requires NMDAR activation and PDZ-dependent interactions, these requirements can be overcome by overexpression of the recombinant protein.

The depression of basal synaptic responses produced by PTEN might be a consequence of an abnormal cycling of

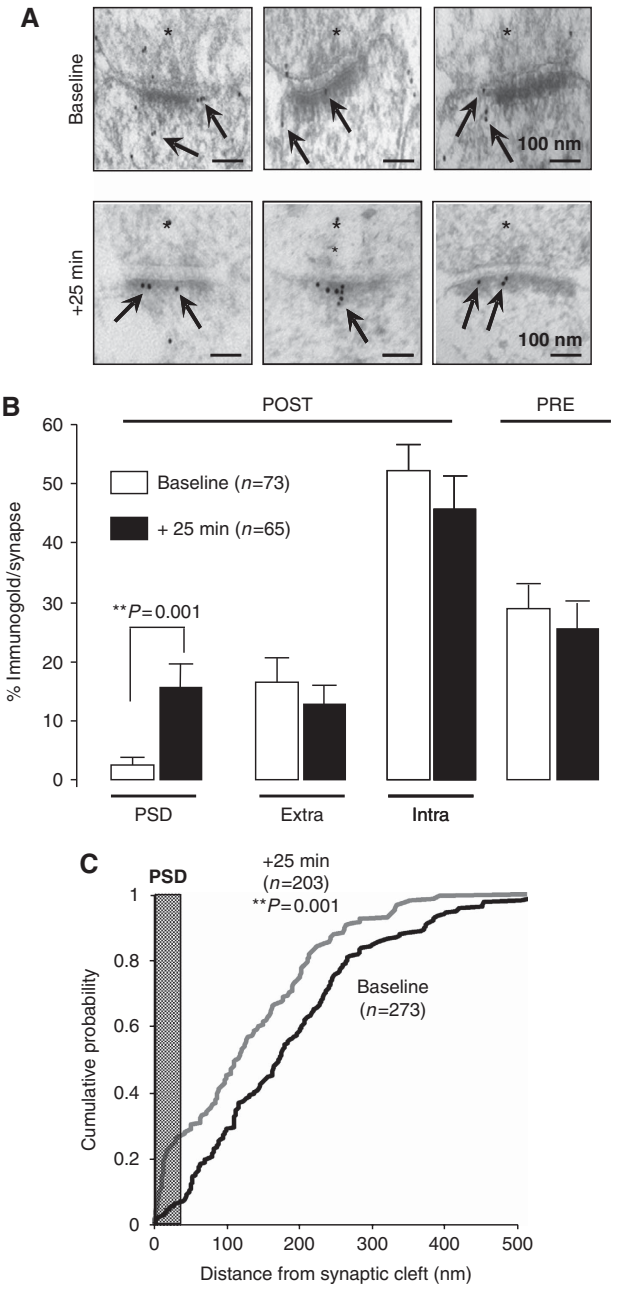


**Figure 4** Local redistribution of PTEN to the postsynaptic density after NMDA receptor activation. (**A**) Representative micrographs of CA1 stratum radiatum excitatory synapses after postembedding labelling with anti-PTEN immunogold (arrows). Presynaptic terminal is marked with an asterisk (*). Note accumulation of PTEN labelling at the PSD after 5 min NMDA treatment and 25 min recovery in ACSF ('+25 min'), with respect to untreated slices ('Baseline'). (**B**) Quantification of PTEN immunogold labelling at different compartments from electron micrographs as the ones shown in (**A**). 'PRE': presynaptic terminal; 'POST': postsynaptic terminal; 'PSD': postsynaptic density; 'Extra': perisynaptic membrane lateral from the PSD; 'Intra': intracellular space within the spine. Percentage of immunogold labelling per synapse was calculated as the number of gold particles at each compartment divided by the total number of gold particles in each synaptic terminal (only gold particles within 1 μm of the synaptic membrane were used for this analysis). Average values ± s.e.m. are plotted for untreated slices ('Baseline', white columns) or for slices treated for 5 min with NMDA and recovered for 25 min in ACSF ('+25 min', black columns); '*n*' represents number of synaptic terminals. Statistical significance was calculated according to the Mann–Whitney test. (**C**) Quantification of PTEN distribution within the spine. The distance to the synaptic cleft was calculated for each immunogold particle before ('Baseline', black line) or after NMDA treatment ('+25 min', grey line), and plotted as cumulative distributions. The average thickness of the PSD from our micrographs (37 nm) is indicated in the plot as a vertical grey bar; '*n*' represents number of gold particles. Statistical significance was calculated according to the Kolmogorov–Smirnov test.

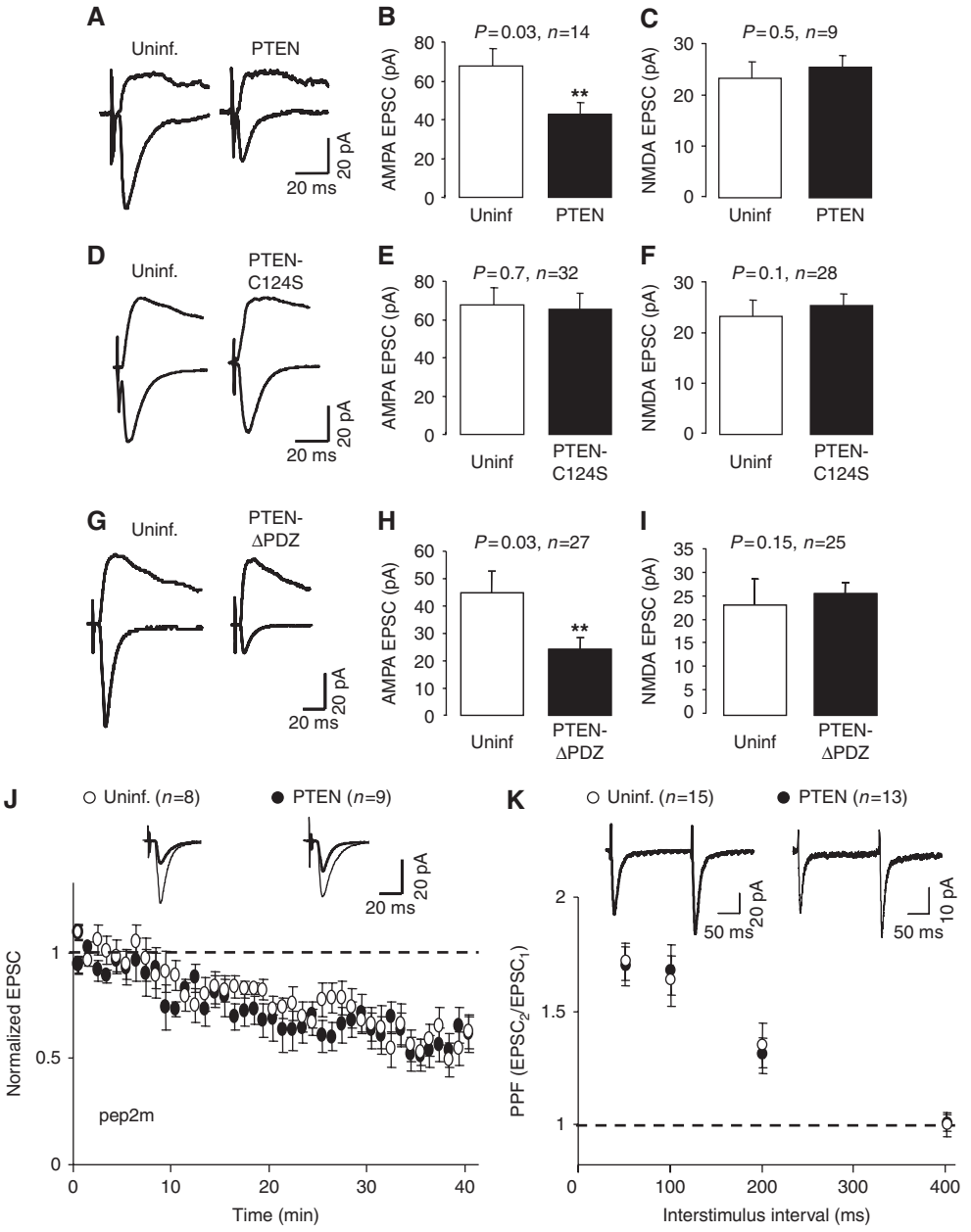


**Figure 5** Effects of GFP-PTEN expression on synaptic transmission. (**A**) Sample traces of evoked AMPAR- and NMDAR-mediated synaptic responses recorded at −60 or +40 mV, respectively, from CA1 neurons expressing GFP-PTEN and neighbouring control (uninfected) neurons. (**B**) Average AMPAR-mediated current amplitude (peak of the synaptic response recorded at −60 mV) from pairs of uninfected and GFP-PTEN-expressing neurons. For (**B**, **C**, **E**, **F**, **H**, **I**), '*n*' represents number of pairs of cells, and statistical significance was determined with the Wilcoxon's test for paired data. (**C**) Average NMDAR-mediated current amplitude (recorded at +40 mV and measured at a latency of 60 ms) from pairs of uninfected and GFP-PTEN-expressing neurons. (**D–F**) Similar to (**A–C**), with infected neurons expressing GFP-PTEN-C124S. (**G–I**) Similar to (**A–C**), with infected neurons expressing GFP-PTEN-ΔPDZ. (**J**) Time course of AMPAR-mediated synaptic responses recorded from CA1 neurons expressing GFP-PTEN or from control (uninfected) neurons, during whole-cell pipette infusion of the GluA2-NSF interfering peptide (pep2 m). Response amplitude is normalized to a 2 min baseline from the beginning of the recording; '*n*' represents number of cells. Inset: sample traces averaged from the first 5 min of the recording (thin lines) or from the last 5 min of the time course (thick lines). (**K**) Paired-pulse facilitation (PPF) recorded from control (uninfected) neurons or from neurons expressing GFP-PTEN. PPF is calculated as the ratio of the amplitude of the second response versus that of the first one; '*n*' represents number of cells. Inset: representative traces of evoked AMAR-mediated responses with an interstimulus interval of 200 ms.

AMPARs at synapses. AMPARs are believed to cycle continuously in and out of synapses in an activity-independent manner, which depends on the interaction between the GluA2 subunit (also known as GluR2;Collingridge *et al*, 2009) and NSF (*N*-ethylmaleimide-sensitive fusion protein) (Nishimune *et al*, 1998; Song *et al*, 1998; Luscher *et al*, 1999). When this interaction is impaired by intracellular infusion of a peptide containing the NSF-binding sequence of GluA2 (pep2m/G10), AMPAR-mediated synaptic transmission rapidly 'runs down' as the receptors continue to be internalized, but fail to be reinserted at the synaptic membrane (Nishimune *et al*, 1998; Luscher *et al*, 1999). We have used the same approach to determine whether PTEN affects the constitutive cycling of AMPA receptors. To this end, we

recorded AMPAR-mediated synaptic responses from CA1 hippocampal neurons infected with PTEN, whereas infusing them with the GluA2-NSF peptide pep2m/G10. The peptide produced a fast 'run-down' of synaptic transmission in the uninfected cells (Figure 5J, white symbols), as expected. This 'run-down' was virtually identical in the cells expressing PTEN (Figure 5J, black symbols), indicating that PTEN activity does not alter the continuous cycling of AMPARs.

Although PTEN was expressed in postsynaptic CA1 neurons, we examined whether presynaptic properties may have been altered retrogradely (Regalado *et al*, 2006; Futai *et al*, 2007). As shown in Figure 5K, paired-pulse facilitation (PPF), an indicator of presynaptic function, was unaltered by PTEN overexpression.

The $PIP_3$ pathway is also involved in the regulation of gene expression (Brunet *et al*, 2001). Nevertheless, overnight overexpression of PTEN did not affect the expression levels of GluA1 and GluA2 subunits of AMPA receptors, or their phosphorylation state (phospho-Ser 831 and 845 for GluA1, and phospho-Ser 880 for GluA2; Supplementary Figure 5).

Therefore, these combined data strongly suggest that PTEN has a specific postsynaptic function at excitatory hippocampal synapses.

### *PTEN activity is required for NMDA receptor-dependent LTD*

The depression of AMPAR responses as a consequence of PTEN overexpression led us to think that this phosphatase may have a function in long-lasting changes of synaptic strength, and particularly, in LTD. In addition, the NMDA treatments that we found to regulate the association of PTEN with postsynaptic elements (Figures 1 and 3) and its redistribution in spines (Figures 2 and 4) are known to lead to synaptic depression (Lee *et al*, 1998).

To directly test a potential function of PTEN in LTD in hippocampal slices, we used a bis-peroxivanadium derivative, bpV(HO)pic, which has been shown to specifically inhibit PTEN when used at a low nanomolar concentrations (Schmid *et al*, 2004) (see Supplementary Figure 6 for a test of bpV(HO)pic specificity). LTD was induced on control or on bpV(HO)pic-pretreated slices by pairing presynaptic stimulation (1 Hz, 500 pulses) with moderate postsynaptic depolarization (−40 mV). Interestingly, when compared with control cells, inhibition of PTEN with bpV(HO)pic greatly reduced the magnitude of LTD (Figure 6A and D), suggesting that PTEN activity is necessary for LTD in CA1 hippocampal synapses (bpv(HO)pic did not have significant effect on the

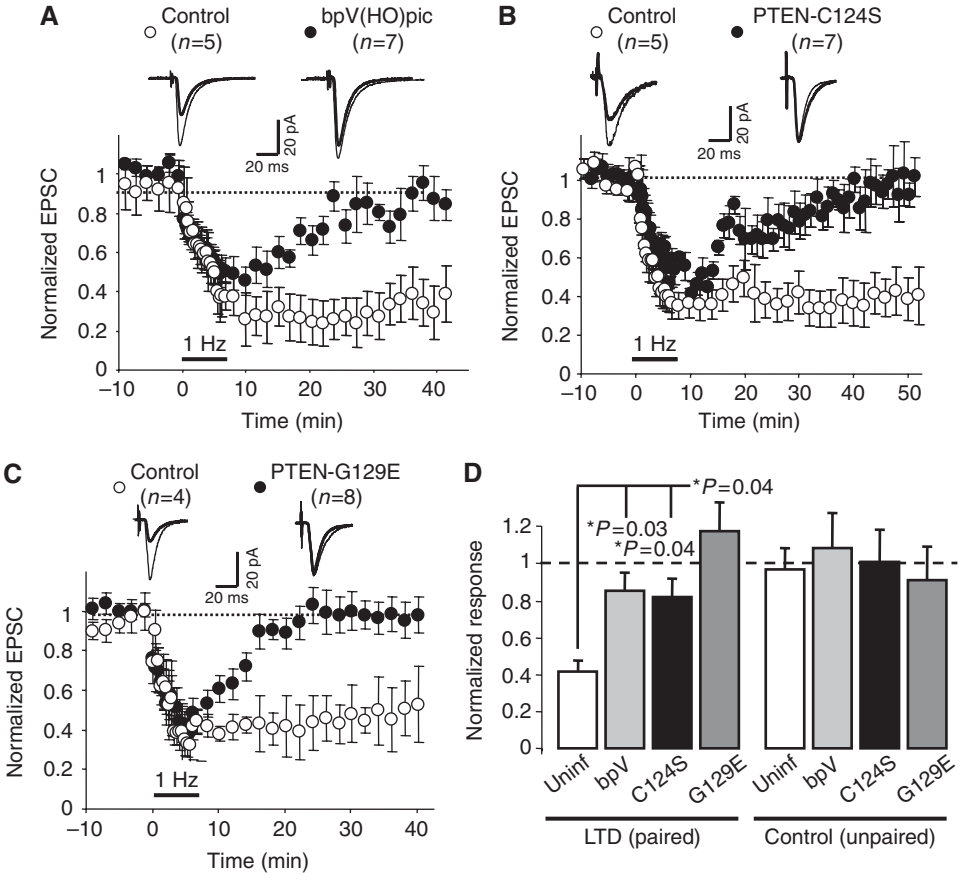


**Figure 6** PTEN lipid phosphatase activity is required for LTD. (**A**–**C**) LTD was induced in CA1 hippocampal neurons pretreated with the PTEN inhibitor bpV(HO)pic (**A**) or expressing the PTEN point mutants C124S (**B**) or G129E (**C**). The results from control neurons (uninfected or untreated) were carried out in an interleaved manner with their corresponding infected or treated neurons. Amplitude of the synaptic responses is normalized to a 10 min baseline. Insets: sample traces averaged from the baseline (thin lines) or from the last 10 min of the recording (thick lines). (**D**) Average of AMPAR-mediated responses collected from the last 10 min of the recording and normalized to the baseline. Left columns (LTD, paired) correspond to the stimulation pathway in which postsynaptic depolarization (−40 mV) was paired to low-frequency stimulation (1 Hz). Right columns (control, unpaired) correspond to the pathway that was not stimulated during depolarization; '*n*' represents number of cells.

 

control pathway—Figure 6D—or on basal synaptic transmission—not shown). Similar blockade of LTD expression was observed when the PTEN inhibitor was applied only during the time of LTD induction (see Supplementary Figure 7).

As an alternative approach to test the function of PTEN in LTD, we carried out similar experiments with neurons expressing the catalytically dead mutant PTEN-C124S. It is important to keep in mind that this mutant did not have any effect on basal AMPAR- or NMDAR-mediated transmission (Figure 5D–F). Interestingly, PTEN-C124S displayed a dominant negative effect on LTD. That is, PTEN-C124S expression blocked LTD to a similar extent as the PTEN inhibitor (Figure 6B and D).

PTEN is known to have both lipid and protein phosphatase activity, as well as phosphatase-independent functions (Tamguney and Stokoe, 2007). To test whether the function of PTEN in LTD was specifically dependent on its $PIP_3$-phosphatase activity, we used a lipid phosphatase PTEN mutant that retains its protein phosphatase activity: PTEN-G129E (Myers *et al*, 1998). Similar to our results with PTEN-C124S, neurons expressing PTEN-G129E did not undergo long-lasting depression (Figure 6C and D). Taken together, these pharmacological and genetic approaches indicate that PTEN lipid phosphatase activity is required for LTD in CA1 hippocampal synapses.

To further explore the function of PTEN in synaptic depression, we evaluated LTD in neurons overexpressing wild-type PTEN. As shown in Supplementary Figure 8, PTEN overexpression did not alter LTD expression. Taking into account that PTEN-overexpressing neurons display reduced AMPAR-mediated synaptic transmission under basal conditions (Figure 5A and B), these data suggest either that PTEN-induced depression does not saturate subsequent LTD expression, or, alternatively, that overexpressed PTEN acts on a different pool of AMPARs from those removed during synaptically induced LTD.

### *PTEN is neither required for LTP nor for metabotropic glutamate receptor-dependent LTD*

After having established the importance of PTEN for LTD, we wished to investigate whether PTEN activity is required for LTP, another paradigmatic form of NMDAR-dependent synaptic plasticity. To this end, we evaluated the effect of the catalytically dead mutant, PTEN-C124S, on LTP in CA1 hippocampal neurons. LTP was induced on infected and uninfected CA1 neurons by pairing presynaptic stimulation (3 Hz, 300 pulses) with postsynaptic depolarization (0 mV). As shown in Figure 7A and C, no significant difference was found between uninfected (control) and infected (PTEN-C124S-expressing) neurons. PTEN-C124S did not have any effect on the non-potentiated (unpaired) pathway either (Figure 7C). Virtually identical results were obtained with the specific PTEN inhibitor bpV(HO)pic (Figure 7B and C). Therefore, these data indicate that PTEN is required specifically for LTD, and not for other forms of NMDAR-dependent synaptic plasticity.

In addition, we tested whether PTEN would be required for another prominent form of LTD in CA1 hippocampal synapses, which is dependent on the activation of metabotropic glutamate receptors (mGluRs) (Oliet *et al*, 1997; Palmer *et al*, 1997). mGluR-dependent LTD was induced by bath application of 50 μM DHPG (group I mGluR agonist) in the presence of 100 μM AP5 (NMDAR antagonist) (see Materials and methods). As shown in Figure 7D and F, neurons expressing the catalytically dead PTEN-C124S displayed similar depression to the control, uninfected neurons. Again, identical results were obtained when blocking PTEN activity pharmacologically (Figure 7E and F). Therefore, we conclude that PTEN is not required for mGluR-dependent LTD in CA1 neurons.

### *Involvement of PDZ-dependent interactions of PTEN during NMDAR-dependent LTD*

Our electrophysiological data shown above indicate that PTEN activity is specifically required for NMDAR-dependent LTD, but not for basal synaptic transmission or other forms of synaptic plasticity. In part, these conclusions are based on the observation that catalytically inactive forms of PTEN have a dominant negative effect on endogenous PTEN to block NMDAR-dependent LTD (Figure 6B and C). In other words, these PTEN mutants appear to be competing with endogenous PTEN for some important interaction required for LTD. An obvious candidate for this interaction is the PDZ motif at the C-terminus of PTEN, which we have found to mediate the anchoring of PTEN in the spine and its association with PSD-95 upon NMDAR activation (Figure 2).

To investigate whether PDZ-dependent interactions of PTEN are important for its function in LTD, we tested whether the dominant negative effect of PTEN-C124S requires its PDZ C-terminal motif. To this end, we generated a catalytically dead mutant (C124S) lacking the PDZ ligand motif (-ITKV*). This mutant (PTEN-C124S-ΔPDZ) did not affect basal synaptic transmission mediated by AMPA or NMDA receptors (Figure 8A–C), consistent with the results with PTEN-C124S (Figure 5D–F). Then, we carried out LTD experiments in CA1 neurons expressing this truncated, catalytically dead mutant. Interestingly, neurons expressing PTEN-C124S-ΔPDZ displayed normal LTD, undistinguishable from uninfected cells (Figure 8D and E). Therefore, these results suggest that the C-terminal PDZ-binding motif of PTEN is necessary for its function in LTD.

## Discussion

In this study, we show that the lipid phosphatase PTEN, typically associated with cell growth and proliferation, is recruited to synapses and is required for the expression of NMDAR-dependent LTD. This is based on three main lines of evidence. First, using electrophysiological assays on hippocampal slices, we have determined that enhancement of PTEN activity is sufficient to depress AMPAR-mediated synaptic transmission, and that PTEN lipid phosphatase activity is specifically required for NMDAR-dependent LTD. Second, a combination of live imaging, electron microscopy and biochemical assays indicate that NMDAR activation triggers a PDZ-dependent association between PTEN and the synaptic scaffold, which anchors PTEN at the postsynaptic terminal. And third, this PDZ-dependent interaction appears to be involved in PTEN's action during LTD, as a dominant negative mutant of PTEN is ineffective when lacking its PDZ motif. These combined results reveal PTEN as a regulated signalling molecule at synapses, which is recruited to the postsynaptic membrane in an activity-dependent manner and

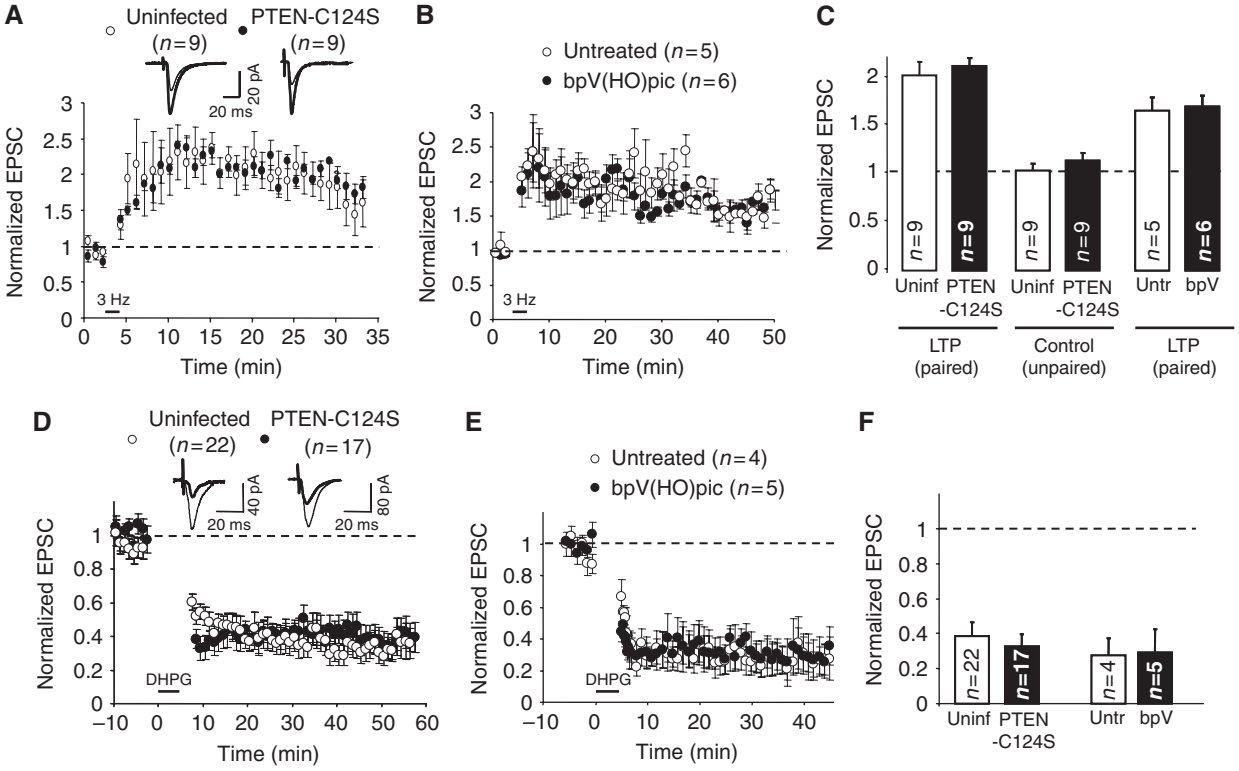


**Figure 7** PTEN activity is not required for LTP or for mGluR-dependent LTD. (**A**) LTP was induced in CA1 hippocampal neurons expressing GFP-PTEN-C124S (black symbols) or in control (uninfected) neurons (white symbols). Amplitude of the synaptic response is normalized to a 2 min baseline. Inset: sample traces averaged from the baseline (thin lines) or from the last 10 min of the recording (thick lines). (**B**) Similar to (**A**), using slices pretreated with the PTEN inhibitor bpV(HO)pic or control (untreated) slices. (**C**) Average of AMPAR-mediated responses collected from the last 10 min of the recording (25–35 min in (**A**), 40–50 min in (**B**)) and normalized to the baseline. Left and right columns (LTP, paired) correspond to the stimulation pathway in which postsynaptic depolarization (0 mV) was paired to presynaptic stimulation (3 Hz). Middle columns (control, unpaired) correspond to the pathway that was not stimulated during depolarization; '*n*' represents number of cells. (**D**) mGluR-dependent LTD was induced by bath application of 50 μM DHPG (agonist of type I mGluR receptors). Recordings were carried out in the presence of 100 μM AP5 (NMDAR antagonist) (see Materials and methods). Synaptic responses were normalized to a 10 min baseline before DHPG application for uninfected neurons (white symbols) and for GFP-PTEN-C124S-expressing neurons (black symbols). Inset: sample traces averaged from the baseline (thin lines) or from the last 10 min of the recording (thick lines). (**E**) Similar to (**D**), using slices pretreated with the PTEN inhibitor bpV(HO)pic or control (untreated) slices. (**F**) Average of AMPAR-mediated responses collected from the last 10 min of the recording (50–60 min in (**D**), 35–45 in (**E**)) and normalized to the baseline.

is required for the modulation of synaptic activity during plasticity.

An important aspect of this work is the identification of a precise synaptic function for PTEN during plasticity. PTEN is a well-known negative regulator of PI3K signalling, and as such, it controls multiple aspects of neuronal development, including neurite growth, axon specification, dendritic arborization and growth cone dynamics (Jaworski *et al*, 2005; Chadborn *et al*, 2006; Kwon *et al*, 2006). In this context, it may not be surprising that earlier studies using heterozygous or mosaic PTEN knock-out mice have reported multiple impairments in synaptic function, including basal transmission, PPF, LTP and LTD (Wang *et al*, 2006; Fraser *et al*, 2008). These complex phenotypes are probably related to general neuronal dysfunctions caused by alterations in the $PIP_3$ pathway during development. Our data presented here indicate that semi-acute (15–20 h) blockade of PTEN activity, either through pharmacological or genetic approaches, results in a very specific impairment of NMDAR-dependent LTD, without affecting basal synaptic transmission, NMDAR function, LTP, mGluR-dependent LTD or presynaptic function. Therefore, we believe that these results are revealing an acute and distinct function of PTEN at otherwise unperturbed synapses.

Perhaps one of the most surprising observations of this study is the recruitment of PTEN to the postsynaptic complex in response to NMDAR activation. PTEN was already known to interact with PDZ domain-containing proteins in different cell types (Bonifant *et al*, 2007). However, no such interaction had been reported in neurons before this work. We now identify PSD-95 as a potential PDZ synaptic partner for PTEN. This association is very low under basal conditions, but it is rapidly triggered upon NMDAR activation. We should also point out that our results do not prove a direct interaction between PTEN and PSD-95. Given the dense network of interactions present at the postsynaptic membrane, it is possible that the association between PTEN and PSD-95 is just reflecting the recruitment of PTEN to the postsynaptic scaffold. Indeed, this recruitment may be maintained by different sets of interactions at different time points, as the anchoring of PTEN in spines and its presence at the PSD (fluorescence and electron microscopy data) appears to be longer lasting than its association with PSD-95 (co-immunoprecipitations). This interpretation would also fit with earlier reports showing that PSD-95 is partially removed from spines during LTD (Horne and Dell'Acqua, 2007; Bhattacharyya *et al*, 2009; Sturgill *et al*, 2009).

 

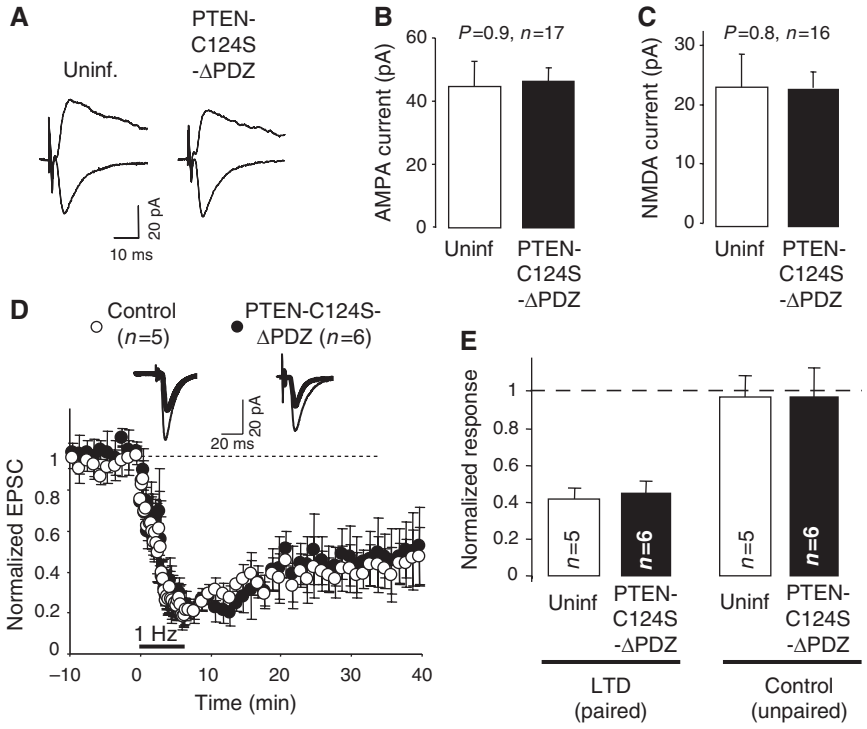


**Figure 8** Involvement of the PDZ motif of PTEN in LTD. (**A**) Sample traces of evoked AMPAR- and NMDAR-mediated synaptic responses recorded at −60 or +40 mV, respectively, from CA1 neurons expressing GFP-PTEN-C124S-ΔPDZ and neighbouring control (uninfected) neurons. (**B**) Average AMPAR-mediated current amplitude (peak of the synaptic response recorded at −60 mV) from pairs of uninfected and GFP-PTEN-C124S-ΔPDZ-expressing neurons. For (**B**) and (**C**), '*n*' represents number of pairs of cells, and statistical significance was determined with the Wilcoxon's test. (**C**) Average NMDAR-mediated current amplitude (recorded at +40 mV and measured at a latency of 60 ms) from pairs of uninfected and GFP-PTEN-C124S-ΔPDZ-expressing neurons. (**D**) LTD was induced in CA1 hippocampal neurons expressing GFP-PTEN-C124S-ΔPDZ (black symbols) or in control (uninfected) neurons (white symbols). Amplitude of the synaptic responses is normalized to a 10 min baseline. Insets: sample traces averaged from the baseline (thin lines) or from the last 10 min of the recording (thick lines). (**E**) Average of AMPAR-mediated responses collected from the last 10 min of the recording and normalized to the baseline. Left columns (LTD, paired) correspond to the stimulation pathway in which postsynaptic depolarization (−40 mV) was paired to low-frequency stimulation (1 Hz). Right columns (control, unpaired) correspond to the pathway that was not stimulated during depolarization; '*n*' represents number of cells.

The regulation of PTEN interactions during LTD is likely to occur at multiple levels. For example, we have observed that NMDAR activation triggers a transient mobilization of PTEN within dendritic spines, which precedes its PDZ-dependent anchoring. Therefore, it is likely that the regulation of PTEN in response to NMDAR activation will involve release from basal retention interactions, as well as association with new synaptic partners. In fact, the initial mobilization of PTEN may facilitate its subsequent association with PSD-95 at the PSD. Undoubtedly, further work will be required to dissect the details of this dynamic behaviour of PTEN within dendritic spines. Nevertheless, these new results strengthen the emerging notion that PSD-95 acts as an important organizer of synaptic signalling during LTD (Xu *et al*, 2008; Bhattacharyya *et al*, 2009).

What are the functional consequences of this activity-dependent recruitment of PTEN to the postsynaptic complex? It is reasonable to hypothesize that binding of PTEN to the postsynaptic complex positions PTEN in close proximity to the postsynaptic membrane, which in turn would facilitate access to its $PIP_3$ substrate during NMDAR-dependent LTD. On the one hand, the stabilization of PTEN in close proximity to its substrate could have significant effects on its catalytic efficiency. But perhaps more importantly, this mechanism would also restrict PTEN action to the postsynaptic membrane of the synapses being activated. In other words, this regulated PDZ-dependent recruitment of PTEN may provide the means to achieve synapse-specific modulation of $PIP_3$ signalling during plasticity.

And finally, how does PTEN activity lead to LTD expression? We have recently described that downregulation of $PIP_3$ leads to the redistribution of AMPARs from the postsynaptic membrane into the extrasynaptic surface of the spine (Arendt *et al*, 2010). On the one hand, this short-range movement is expected to depress synaptic transmission, as perisynaptic AMPARs will not be significantly activated by synaptically released glutamate (Raghavachari and Lisman, 2004). On the other hand, this redistribution of AMPARs may facilitate their access to perisynaptic endocytic hotspots (Blanpied *et al*, 2002; Petralia *et al*, 2003; Racz *et al*, 2004), and, therefore, may act as an initial step preceding AMPAR internalization.

A downstream effector of the $PIP_3$ pathway is glycogen synthase kinase-3 β (GSK-3β). Upregulation of $PIP_3$ levels leads to activation of the Ser/Thr kinase Akt, which in turn phosphorylates and inactivates GSK-3β (Cross *et al*, 1995). Therefore, PTEN will act as a positive regulator of GSK-3β, by reducing $PIP_3$ levels with the concomitant decrease in Akt activation and dephosphorylation (activation) of GSK-3β. Interestingly, GSK-3β has been recently shown to be activated (dephosphorylated) upon LTD induction, and this activation was required for the specific expression of LTD (versus LTP) (Peineau *et al*, 2007). Therefore, it is possible that the

recruitment of PTEN to the postsynaptic membrane during LTD is relayed through the $PIP_3$ pathway to activate GSK-3β at specific synapses. This mechanism would be consistent with the presence of GSK-3β in synaptosomal preparations and dendritic spines (Hooper *et al*, 2007; Peineau *et al*, 2007). Therefore, our results propose a specific mechanism for the synaptic compartmentalization of $PIP_3$ signalling during plasticity.

In addition, it has been recently shown that LTD requires $PIP_2$ turnover by phospholipase C (PLC), which leads to the loss of the scaffolding molecules AKAP79 and PSD-95 from synapses and initiates the structural remodelling of the spine (Horne and Dell'Acqua, 2007). Taking together, Dell'Acqua's study and ours would suggest an interesting relay of phosphoinositide metabolism during LTD, which would involve degradation of $PIP_3$ into $PIP_2$ (through PTEN) for initial AMPAR depression, and subsequent $PIP_2$ turnover (through PLC) for further structural and functional changes in the spine.

In summary, this work has offered new insights into the organization of synaptic signalling during plasticity and has revealed distinct functions for the tumour suppressor PTEN as a critical mediator of LTD in hippocampal neurons.

## Materials and methods

Expression of recombinant proteins and antibodies used in this study are described in Supplementary data.

### *Co-immunoprecipitations and pharmacological treatments*

Hippocampal slices were transferred to a submersion-type holding chamber containing artificial cerebrospinal fluid (ACSF, composition described in Supplementary data), gassed with 5% $CO_2$/95% $O_2$ at 30°C. Slices were equilibrated in the holding chamber for 10 min before each experiment and were transferred to a separate chamber containing ACSF plus 20 μM NMDA, 100 μM AMPA or 50 mM KCl, in which they remained for 5 min. After these treatments, some slices were taken immediately for homogenization in a buffer containing 10 mM HEPES, 150 mM NaCl, 10 mM EDTA, 0.1 mM phenylmethanesulphonylfluoride, 2 μg/ml of chymostatin, leupeptin, anti-pain and pepstatin, 10 mM NaF, 1 μM microcystin LR, 0.5 μM calyculin A and 1% Triton X-100. Other slices were transferred to another chamber containing ACSF, for variable recovery times, as indicated in each experiment. Total protein extracts were prepared in the buffer described above. For immunoprecipitations, 200–300 μg of protein extracts were incubated with the corresponding antibodies and with 40 μl of protein G-sepharose beads (50%) (Amersham Biosciences) for 4 h at 4°C. These samples were then washed and immunoprecipitated proteins were eluted by boiling in 1x Laemmli sample buffer and separated by SDS–PAGE. Visualization of immunoprecipitated proteins was performed by western blot developed with chemiluminescence or with the Odyssey fluorescence system, and quantified with Image J under linear conditions.

### *Electrophysiology*

Voltage-clamp whole-cell recordings were obtained from nearby infected and uninfected CA1 pyramidal neurons, under visual guidance using fluorescence and transmitted light illumination. Composition of ACSF and internal solution and description of synaptic plasticity protocols are included in Supplementary data. Bipolar stimulating electrodes were placed over Schaffer collateral fibres between 250 and 300 μm from the CA1 recorded cells, and synaptic responses were evoked with single voltage pulses (200 μs, up to 30 V). Responses were collected at −60 and +40 mV and averaged over 50–100 trials. All electrophysiological data were collected with pCLAMP software (Molecular Devices).

### *Fluorescence recovery after photobleaching*

Hippocampal slices (5–7 DIV) were perfused with ACSF for 15–30 min. Confocal images of dendritic spines were obtained on an Olympus FV500 confocal microscope using a 60× oil immersion objective. Digital images were acquired using the FluoView software. After acquisition of baseline images, dendritic spines were photobleached for 5 s (approximate time to completely bleach fluorescence signal in the spine). Recovery of fluorescence in the spine was measured from images acquired up to 50 s after the photobleaching. After collecting several images from dendritic spines under baseline conditions, the perfusion solution was switched to an ACSF containing 20 μM NMDA. After 5 min of NMDA treatment, the slices were washed again with standard ACSF. Further FRAP images were acquired after 10, 20 and 30 min of the NMDA treatment. Images were reconstructed and analysed using NIH Image J software.

### *Electron microscopy*

Rat hippocampus was fixed, dehydrated and processed for postembedding immunogold labelling as earlier described (Phend *et al*, 1995). Immunostaining was done with anti-PTEN antibody (Neomarkers) followed by an anti-mouse secondary antibody coupled to 10 nm gold particles (Electron Microscopy Sciences). Images were acquired with a Philips CM-100 transmission electron microscope coupled to a Kodak 1.6 Megaplus digital camera. Quantification of gold particles and distance measurements were carried out on the digital images using NIH Image J software.

### *Statistical analysis*

Statistical differences were calculated according to non-parametric tests. Comparisons between multiple groups were carried out with the Kruskal–Wallis ANOVA. When significant differences were observed, *P*-values for pairwise comparisons were calculated according to two-tailed Mann–Whitney tests (for unpaired data) or Wilcoxon's tests (for paired data). Comparisons between cumulative distributions (Figure 4C) were calculated with the Kolmogorov–Smirnov test.

### *Supplementary data*

Supplementary data are available at *The EMBO Journal* Online (http://www.embojournal.org).

## Acknowledgements

We thank Kristin Arendt and members of the Esteban laboratory for their critical reading of this paper. We also thank MD Ledesma for her advice with the synaptosomal preparations. The monoclonal antibody against PSD-95 was developed by and obtained from the UC Davis/NIH NeuroMab Facility, supported by NIH grant U24NS050606 and maintained by the Department of Neurobiology, Physiology and Behavior, College of Biological Sciences, University of California, Davis, CA 95616. This work was supported by grants from the National Institute of Mental Health (MH070417) and the Spanish Ministry of Science and Innovation (SAF-2008-04616, SAF-2009-05558-E) to JAE. MB, SK and AL are supported by the Spanish Ministry of Science and Innovation. MB is also the recipient of an award from the Fondation Bettencourt-Schuller (France).

## Conflict of interest

The authors declare that they have no conflict of interest.

## References

Arendt KL, Royo M, Fernandez-Monreal M, Knafo S, Petrok CN, Martens JR, Esteban JA (2010) PIP3 controls synaptic function by maintaining AMPA receptor clustering at the postsynaptic membrane. *Nat Neurosci* **13:** 36–44

Backman SA, Stambolic V, Suzuki A, Haight J, Elia A, Pretorius J, Tsao MS, Shannon P, Bolon B, Ivy GO, Mak TW (2001) Deletion of Pten in mouse brain causes seizures, ataxia and defects in soma size resembling Lhermitte-Duclos disease. *Nat Genet* **29:** 396–403

 

Bhattacharyya S, Biou V, Xu W, Schluter O, Malenka RC (2009) A critical role for PSD-95/AKAP interactions in endocytosis of synaptic AMPA receptors. *Nat Neurosci* **12:** 172–181

Blanpied TA, Scott DB, Ehlers MD (2002) Dynamics and regulation of clathrin coats at specialized endocytic zones of dendrites and spines. *Neuron* **36:** 435–449

Bonifant CL, Kim JS, Waldman T (2007) NHERFs, NEP, MAGUKs, and more: interactions that regulate PTEN. *J Cell Biochem* **102:** 878–885

Brunet A, Datta SR, Greenberg ME (2001) Transcription-dependent and -independent control of neuronal survival by the PI3K-Akt signaling pathway. *Curr Opin Neurobiol* **11:** 297–305

Butler MG, Dasouki MJ, Zhou XP, Talebizadeh Z, Brown M, Takahashi TN, Miles JH, Wang CH, Stratton R, Pilarski R, Eng C (2005) Subset of individuals with autism spectrum disorders and extreme macrocephaly associated with germline PTEN tumour suppressor gene mutations. *J Med Genet* **42:** 318–321

Cammalleri M, Lutjens R, Berton F, King AR, Simpson C, Francesconi W, Sanna PP (2003) Time-restricted role for dendritic activation of the mTOR-p70S6K pathway in the induction of late-phase long-term potentiation in the CA1. *Proc Natl Acad Sci USA* **100:** 14368–14373

Carlin RK, Grab DJ, Cohen RS, Siekevitz P (1980) Isolation and characterization of postsynaptic densities from various brain regions: enrichment of different types of postsynaptic densities. *J Cell Biol* **86:** 831–845

Chadborn NH, Ahmed AI, Holt MR, Prinjha R, Dunn GA, Jones GE, Eickholt BJ (2006) PTEN couples Sema3A signalling to growth cone collapse. *J Cell Sci* **119:** 951–957

Chen X, Garelick MG, Wang H, Lil V, Athos J, Storm DR (2005) PI3 kinase signaling is required for retrieval and extinction of contextual memory. *Nat Neurosci* **8:** 925–931

Collingridge GL, Olsen RW, Peters J, Spedding M (2009) A nomenclature for ligand-gated ion channels. *Neuropharmacology* **56:** 2–5

Cross DA, Alessi DR, Cohen P, Andjelkovich M, Hemmings BA (1995) Inhibition of glycogen synthase kinase-3 by insulin mediated by protein kinase B. *Nature* **378:** 785–789

Ehrlich I, Malinow R (2004) Postsynaptic density 95 controls AMPA receptor incorporation during long-term potentiation and experience-driven synaptic plasticity. *J Neurosci* **24:** 916–927

El-Husseini AE, Schnell E, Chetkovich DM, Nicoll RA, Bredt DS (2000) PSD-95 involvement in maturation of excitatory synapses. *Science* **290:** 1364–1368

Eng C (2003) PTEN: one gene, many syndromes. *Hum Mutat* **22:** 183–198

Fraser MM, Bayazitov IT, Zakharenko SS, Baker SJ (2008) Phosphatase and tensin homolog, deleted on chromosome 10 deficiency in brain causes defects in synaptic structure, transmission and plasticity, and myelination abnormalities. *Neuroscience* **151:** 476–488

Futai K, Kim MJ, Hashikawa T, Scheiffele P, Sheng M, Hayashi Y (2007) Retrograde modulation of presynaptic release probability through signaling mediated by PSD-95-neuroligin. *Nat Neurosci* **10:** 186–195

Hooper C, Markevich V, Plattner F, Killick R, Schofield E, Engel T, Hernandez F, Anderton B, Rosenblum K, Bliss T, Cooke SF, Avila J, Lucas JJ, Giese KP, Stephenson J, Lovestone S (2007) Glycogen synthase kinase-3 inhibition is integral to long-term potentiation. *Eur J Neurosci* **25:** 81–86

Horne EA, Dell'Acqua ML (2007) Phospholipase C is required for changes in postsynaptic structure and function associated with NMDA receptor-dependent long-term depression. *J Neurosci* **27:** 3523–3534

Jaworski J, Spangler S, Seeburg DP, Hoogenraad CC, Sheng M (2005) Control of dendritic arborization by the phosphoinositide-3′-kinase-Akt-mammalian target of rapamycin pathway. *J Neurosci* **25:** 11300–11312

Kwon CH, Luikart BW, Powell CM, Zhou J, Matheny SA, Zhang W, Li Y, Baker SJ, Parada LF (2006) Pten regulates neuronal arborization and social interaction in mice. *Neuron* **50:** 377–388

Kwon CH, Zhu X, Zhang J, Knoop LL, Tharp R, Smeyne RJ, Eberhart CG, Burger PC, Baker SJ (2001) Pten regulates neuronal soma size: a mouse model of Lhermitte-Duclos disease. *Nat Genet* **29:** 404–411

Lee HK, Kameyama K, Huganir RL, Bear MF (1998) NMDA induces long-term synaptic depression and dephosphorylation of the GluR1 subunit of AMPA receptors in hippocampus. *Neuron* **21:** 1151–1162

Li J, Yen C, Liaw D, Podsypanina K, Bose S, Wang SI, Puc J, Miliaresis C, Rodgers L, McCombie R, Bigner SH, Giovanella BC, Ittmann M, Tycko B, Hibshoosh H, Wigler MH, Parsons R (1997) PTEN, a putative protein tyrosine phosphatase gene mutated in human brain, breast, and prostate cancer. *Science* **275:** 1943–1947

Luscher C, Xia H, Beattie EC, Carroll RC, von Zastrow M, Malenka RC, Nicoll RA (1999) Role of AMPA receptor cycling in synaptic transmission and plasticity. *Neuron* **24:** 649–658

Maehama T, Dixon JE (1998) The tumor suppressor, PTEN/MMAC1, dephosphorylates the lipid second messenger, phosphatidylinositol 3,4,5-trisphosphate. *J Biol Chem* **273:** 13375–13378

Maehama T, Dixon JE (1999) PTEN: a tumour suppressor that functions as a phospholipid phosphatase. *Trends Cell Biol* **9:** 125–128

Myers MP, Pass I, Batty IH, Van der Kaay J, Stolarov JP, Hemmings BA, Wigler MH, Downes CP, Tonks NK (1998) The lipid phosphatase activity of PTEN is critical for its tumor supressor function. *Proc Natl Acad Sci USA* **95:** 13513–13518

Nishimune A, Isaac JT, Molnar E, Noel J, Nash SR, Tagaya M, Collingridge GL, Nakanishi S, Henley JM (1998) NSF binding to GluR2 regulates synaptic transmission. *Neuron* **21:** 87–97

Oliet SH, Malenka RC, Nicoll RA (1997) Two distinct forms of long-term depression coexist in CA1 hippocampal pyramidal cells. *Neuron* **18:** 969–982

Opazo P, Watabe AM, Grant SG, O'Dell, T.J. (2003) Phosphatidylinositol 3-kinase regulates the induction of long-term potentiation through extracellular signal-related kinase-independent mechanisms. *J Neurosci* **23:** 3679–3688

Palmer MJ, Irving AJ, Seabrook GR, Jane DE, Collingridge GL (1997) The group I mGlu receptor agonist DHPG induces a novel form of LTD in the CA1 region of the hippocampus. *Neuropharmacology* **36:** 1517–1532

Peineau S, Taghibiglou C, Bradley C, Wong TP, Liu L, Lu J, Lo E, Wu D, Saule E, Bouschet T, Matthews P, Isaac JT, Bortolotto ZA, Wang YT, Collingridge GL (2007) LTP inhibits LTD in the hippocampus via regulation of GSK3beta. *Neuron* **53:** 703–717

Pendaries C, Tronchere H, Plantavid M, Payrastre B (2003) Phosphoinositide signaling disorders in human diseases. *FEBS Lett* **546:** 25–31

Perandones C, Costanzo RV, Kowaljow V, Pivetta OH, Carminatti H, Radrizzani M (2004) Correlation between synaptogenesis and the PTEN phosphatase expression in dendrites during postnatal brain development. *Brain Res Mol Brain Res* **128:** 8–19

Petralia RS, Wang YX, Wenthold RJ (2003) Internalization at glutamatergic synapses during development. *Eur J Neurosci* **18:** 3207–3217

Phend KD, Rustioni A, Weinberg RJ (1995) An osmium-free method of epon embedment that preserves both ultrastructure and antigenicity for post-embedding immunocytochemistry. *J Histochem Cytochem* **43:** 283–292

Qin Y, Zhu Y, Baumgart JP, Stornetta RL, Seidenman K, Mack V, van Aelst L, Zhu JJ (2005) State-dependent Ras signaling and AMPA receptor trafficking. *Genes Dev* **19:** 2000–2015

Racz B, Blanpied TA, Ehlers MD, Weinberg RJ (2004) Lateral organization of endocytic machinery in dendritic spines. *Nat Neurosci* **7:** 917–918

Raghavachari S, Lisman JE (2004) Properties of quantal transmission at CA1 synapses. *J Neurophysiol* **92:** 2456–2467

Regalado MP, Terry-Lorenzo RT, Waites CL, Garner CC, Malenka RC (2006) Transsynaptic signaling by postsynaptic synapse-associated protein 97. *J Neurosci* **26:** 2343–2357

Sanna PP, Cammalleri M, Berton F, Simpson C, Lutjens R, Bloom FE, Francesconi W (2002) Phosphatidylinositol 3-kinase is required for the expression but not for the induction or the maintenance of long-term potentiation in the hippocampal CA1 region. *J Neurosci* **22:** 3359–3365

Schmid AC, Byrne RD, Vilar R, Woscholski R (2004) Bisperoxovanadium compounds are potent PTEN inhibitors. *FEBS Lett* **566:** 35–38

Sheng M (2001) Molecular organization of the postsynaptic specialization. *Proc Natl Acad Sci USA* **98:** 7058–7061

Song I, Kamboj S, Xia J, Dong H, Liao D, Huganir RL (1998) Interaction of the N-ethylmaleimide-sensitive factor with AMPA receptors. *Neuron* **21:** 393–400

Stambolic V, Suzuki A, de la Pompa JL, Brothers GM, Mirtsos C, Sasaki T, Ruland J, Penninger JM, Siderovski DP, Mak TW (1998) Negative regulation of PKB/Akt-dependent cell survival by the tumor suppressor PTEN. *Cell* **95:** 29–39

Steck PA, Pershouse MA, Jasser SA, Yung WK, Lin H, Ligon AH, Langford LA, Baumgard ML, Hattier T, Davis T, Frye C, Hu R, Swedlund B, Teng DH, Tavtigian SV (1997) Identification of a candidate tumour suppressor gene, MMAC1, at chromosome 10q23.3 that is mutated in multiple advanced cancers. *Nat Genet* **15:** 356–362

Stiles B, Groszer M, Wang S, Jiao J, Wu H (2004) PTENless means more. *Dev Biol* **273:** 175–184

Sturgill JF, Steiner P, Czervionke BL, Sabatini BL (2009) Distinct domains within PSD-95 mediate synaptic incorporation, stabilization, and activity-dependent trafficking. *J Neurosci* **29:** 12845–12854

Tamguney T, Stokoe D (2007) New insights into PTEN. *J Cell Sci* **120:** 4071–4079

Tang SJ, Reis G, Kang H, Gingras AC, Sonenberg N, Schuman EM (2002) A rapamycin-sensitive signaling pathway contributes to long-term synaptic plasticity in the hippocampus. *Proc Natl Acad Sci USA* **99:** 467–472

Valiente M, Andres-Pons A, Gomar B, Torres J, Gil A, Tapparel C, Antonarakis SE, Pulido R (2005) Binding of PTEN to specific PDZ domains contributes to PTEN protein stability and phosphorylation by microtubule-associated serine/threonine kinases. *J Biol Chem* **280:** 28936–28943

Wang Y, Cheng A, Mattson MP (2006) The PTEN phosphatase is essential for long-term depression of hippocampal synapses. *Neuromolecular Med* **8:** 329–336

Wu X, Hepner K, Castelino-Prabhu S, Do D, Kaye MB, Yuan XJ, Wood J, Ross C, Sawyers CL, Whang YE (2000) Evidence for regulation of the PTEN tumor suppressor by a membrane-localized multi-PDZ domain containing scaffold protein MAGI-2. *Proc Natl Acad Sci USA* **97:** 4233–4238

Xu W, Schluter OM, Steiner P, Czervionke BL, Sabatini B, Malenka RC (2008) Molecular dissociation of the role of PSD-95 in regulating synaptic strength and LTD. *Neuron* **57:** 248–262

 